



Effects of adding ethanol to KOH electrolyte on electrochemical performance of titanium carbide-derived carbon



Jiang Xu^a, Ruijun Zhang^{a,*}, Peng Chen^a, Shanhai Ge^{b,**}

^a State Key Laboratory of Metastable Materials Science and Technology, Yanshan University, Qinhuangdao 066004, China

^b Department of Mechanical and Nuclear Engineering, The Pennsylvania State University, University Park, PA 16802, USA

HIGHLIGHTS

- Wettability and contact angle of carbide-derived carbons (CDCs) are investigated.
- Hydrophilicity and specific capacitance of CDC depend on its microstructure.
- Well-ordered graphite ribbons have lower hydrophilicity and capacitance.
- A strategy that improving the surface wettability and capacitive behavior of CDC.

ARTICLE INFO

Article history:

Received 24 June 2013

Received in revised form

13 July 2013

Accepted 16 July 2013

Available online 31 July 2013

Keywords:

Carbide-derived carbon

Supercapacitor

Hydrophilicity

Potassium hydroxide electrolyte

ABSTRACT

Porous carbide-derived carbons (CDCs) are synthesized from TiC at different chlorination temperatures as electrode materials for electrochemical capacitors. It is found that the microstructure of the produced CDCs has significant influence on both the hydrophilicity in aqueous KOH electrolyte and the resultant electrochemical performance. Because the TiC-CDC synthesized at higher temperature (e.g. 1000 °C) contains well-ordered graphite ribbons, it shows lower hydrophilicity and specific capacitance. It is also found that addition of a small amount of ethanol to KOH electrolyte effectively improves the wettability of the CDCs synthesized at higher temperature and the corresponding specific capacitance. Compared with the CDC synthesized at 600 °C, the CDC synthesized at 1000 °C shows fast ion transport and excellent capacitive behavior in KOH electrolyte with addition of ethanol because of the existences of mesopores and high specific surface area.

© 2013 Elsevier B.V. All rights reserved.

1. Introduction

Capacitors and batteries are the most common electrical energy-storage devices. Batteries can provide high energy density but relatively low power density, which restricts their use in a number of applications. Electrochemical capacitors, also known as supercapacitors or ultracapacitors, can provide high specific power (10 kW kg⁻¹), long cycle life (>10⁵), and fast charge/discharge processes (within seconds), and therefore have become an alternative or supplement to batteries in the field of energy storage [1–5]. Recent supercapacitor research and development aim to increase power, energy density, lower fabrication costs and environmentally friendly materials. The electrode materials for

supercapacitors include carbons, conductive polymers, metal oxides, and their composites [6].

Porous carbons as electrode materials for electric double-layer capacitors (EDLCs) have attracted more interest than other materials due to the high specific surface area (SSA), high electrical conductivity, low cost and various forms such as powders, fibers, tubes, and composites etc. [7]. More importantly, carbon materials exhibit high stability in different solutions (from strongly acidic to alkali) in a wide range of temperatures [7]. The electrochemical behavior of the carbon-based supercapacitors is dependent on the SSA. Average pore size and pore size distribution of porous carbon is a key to its capacitance. The capacitance of a carbon-based supercapacitor can be improved significantly by matching the size of solvated electrolyte ions with the pore size distribution of carbon electrode [8–11]. To date, major efforts in the field of carbon-based supercapacitor are to optimize pore size, pore structure and surface properties of the electrode materials.

Carbide derived carbon (CDC) technique is one of the most promising and economic ways to produce carbons with desired

* Corresponding author. Fax: +86 335 8514884.

** Corresponding author.

E-mail addresses: zhangrj@ysu.edu.cn (R. Zhang), sug13@psu.edu (S. Ge).

porosity. CDC is produced by selective removal of metal or metalloid atoms from carbide lattices layer by layer. Atomic-level control can be achieved in the synthesis process, which may produce carbons with pores matching with the size of solvated electrolyte ions [8,12]. Chlorination temperature has a significant influence on the structure of the produced CDC. The pores in CDC can be tuned with subangstrom accuracy in a wide range by controlling the chlorination temperature [12]. The width of the produced pores increases as the chlorination temperature increases [13–16]. In addition, it is notable that the degree of order of the produced CDC increases with increasing chlorination temperature and the microstructure changes from amorphous carbon to graphite ribbons [17–19]. The microstructure of carbon has much influence on both surface properties and conductivity of the carbon-based electrode materials, which greatly affects the resultant electrochemical performance [7,11,20,21]. Although a few efforts have been done on the compatibility of electrolytes with electrodes [8,12,22,23], very few studies in the literature have focused on the microstructure dependence of CDC wettability.

For carbon-based supercapacitors, both organic and aqueous solutions can be used as electrolytes [7,24]. The supercapacitor using organic-based electrolyte can show high performance, but safety, environmental pollution and fabrication cost are big challenges for this kind of supercapacitor. For these reasons, many researches used aqueous electrolytes to improve the performance of hybrid system [25–27]. An eco-friendly and efficient aqueous electrolyte is a key to high performance supercapacitor. Wu et al. [22] reported that carbon electrode in aqueous KOH electrolyte exhibits higher capacitance than neutral aqueous electrolytes because of the fast mobility of OH^- ions.

In our previous work, a microstructure control strategy for CDC by ball-milling metal carbide precursor prior to CDC synthesis was investigated [28]. In this work, the electrochemical performance of the produced CDC is further investigated in aqueous KOH electrolyte. A small amount of ethanol is added to the electrolyte to investigate the effect of wettability of the produced CDC on its electrochemical behaviors.

2. Experimental

2.1. Sample preparation

Commercial available TiC powder (99.5%, $\sim 2 \mu\text{m}$, Changsha Xinlan Cemented Carbide Co. Ltd, P.R. China) was used as precursor. The experimental device has been shown in our previous work [28]. In brief, CDC powder was prepared as follows: TiC powder (approximately 4 g) was placed in a horizontal quartz tube furnace and heated to a desired temperature under argon at atmospheric pressure. Once it reached the desired temperature, the argon flow was stopped and the pure chlorine was passed through the quartz tube at a rate of $\sim 30 \text{ ml min}^{-1}$. Chlorination lasted for 2 h at the desired temperature (e.g. 600, 800, 1000 and 1200°C). In the last step of the experiment, the quartz tube was purged with argon for 30 min to blow away the residual chlorine and chlorides gases, and then cooled down to room temperature under argon flow. The waste gases were adsorbed by NaOH solution.

2.2. Material characterization

Transmission electron microscopy (TEM) was performed using a JEM 2010 TEM equipped with an image filter (Gatan GIF) at 200 kV. A slurry composed of CDC and ethanol was coated on a copper grid with a lacey carbon film to prepare samples for TEM testing. Gas sorption analysis was done by using V-Sorb 2800TP specific surface area and pore size analyzer (Beijing Gold APP Instruments Co. Ltd,

P.R. China) with N_2 as adsorbent at 77 K. Specific surface area – according to BET (Brunauer, Emmet and Teller) theory and nanopore volume – was calculated by using *t*-plots based on the N_2 sorption isotherm. The FTIR measurements were performed on a Fourier transform infrared (FTIR) spectrometer (E55Xfra106, BRUKER, Germany) in the wave range of $1000\text{--}4000 \text{ cm}^{-1}$, using KBr disk method.

2.3. Preparation of electrode and electrochemical measurement

The electrochemical investigation was carried out in a three-electrode system using platinum as counter electrode and Hg/HgO as reference electrode. The working electrodes were prepared as follows: A slurry consisting of 80 wt.% CDC, 10 wt.% carbon black powder and 10 wt.% polytetrafluoroethylene (PTFE, 60 wt.% suspension in water) binder was smeared into nickel foam. Then it was dried in vacuum at 120°C for 12 h. Thereafter, the electrode was pressed at a pressure of 10 Mpa. KOH solutions with/without addition of ethanol were used as electrolyte. The active area of the electrode is 1 cm^2 . Before each measurement, the working electrode was soaked in electrolyte to ensure thoroughly wet.

The electrochemical performances of the produced CDCs were characterized by cyclic voltammetry (CV) in the potential range of $-1.0\text{--}0$ or $-0.8\text{--}0 \text{ V}$ at different scan rates of $20\text{--}500 \text{ mV s}^{-1}$, galvanostatic charge/discharge tests at 500 mA g^{-1} with cutoff voltage of $-1\text{--}0 \text{ V}$ and electrochemical impedance spectroscopy (EIS) in the frequency range from 10^5 Hz to 10^{-2} Hz with amplitude of 5 mV . The CV and EIS measurements were performed on CHI650D electrochemical workstation. The galvanostatic charge/discharge tests were carried out on potentiostat/galvanostat (CT2001A, Land, Wuhan, China).

3. Results and discussion

Fig. 1a and b shows the CVs and galvanostatic charge/discharge curves of TiC-CDCs in 6 M KOH electrolyte, respectively. The CDCs are synthesized at different temperatures. It can be seen from Fig. 1a that all samples exhibit double layer capacitive behavior (rectangular shape) and no faradic reaction can be found within the voltage window. Moreover, the specific capacitance decreases with increasing chlorination temperature. The specific capacitance of CDC synthesized at chlorination temperature of 1000°C (denote as TiC-CDC-1000) decreases to almost zero. The chlorination temperature dependence of specific capacitance of the produced CDC is further confirmed by charge/discharge curves shown in Fig. 1b. It can be found that both curves of the CDCs synthesized at 600 and 800°C (denote as TiC-CDC-600 and TiC-CDC-800) are almost symmetrical isosceles lines, demonstrating that the produced CDCs have typical porous carbon capacitive behavior in 6 M KOH aqueous electrolyte [29]. Whereas for the sample TiC-CDC-1000, both the short charge/discharge time and a sudden potential drop (IR drop) at the beginning of discharge indicate a poor capacitive behavior.

Fig. 2 shows nitrogen adsorption/desorption isotherms of TiC-CDCs synthesized at different temperatures. SSA, average pore size and pore volume is calculated. It shows that TiC-CDC-600 adsorbed N_2 only at low relative pressure (P/P_0), which means that nearly no mesopore exists in this sample (Fig. 2a) [30]. Whereas for TiC-CDC-1000, the uptake of N_2 increases with increasing P/P_0 , indicating a broad pore size distribution in the CDC. Further, a notable hysteresis between N_2 adsorption and desorption isotherms indicates the existence of mesopores in TiC-CDC-1000. Fig. 2b shows that both values of the SSA and pore size increase with increasing chlorination temperature. Large SSA is only a necessary condition for high specific capacitance because the pore size also plays an important role in the achievement of high specific

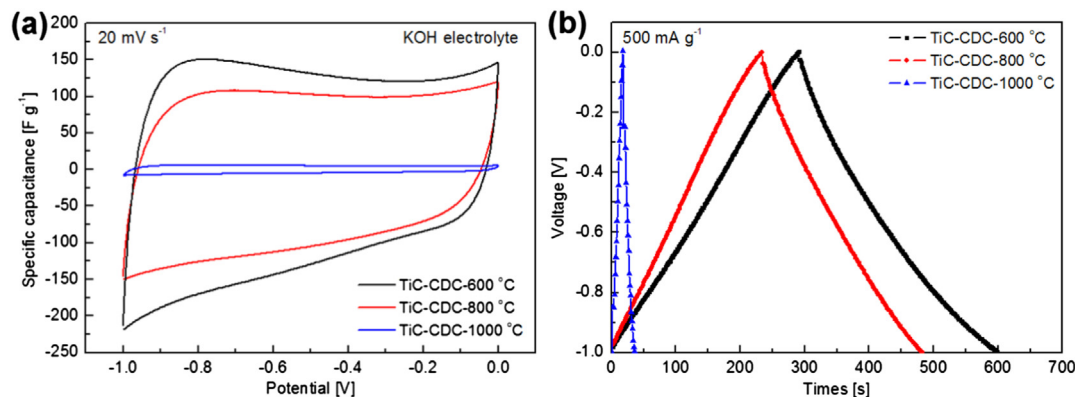


Fig. 1. (a) Cyclic voltammograms (20 mV s⁻¹) and (b) the galvanostatic charging/discharging curves (500 mA g⁻¹) of CDCs in 6 M KOH aqueous electrolyte. The CDCs are synthesized at different temperatures.

capacitance. Chmiola et al. [8] reported that the pores smaller than the size of solvated ions increase the specific capacitance significantly. Although a decrease of specific capacitance of TiC-CDC-1000 has been reported in both organic and H₂SO₄ electrolytes [10,24], the significant decrease detected in aqueous KOH electrolyte has never been reported. The solvated effect cannot lead to such a decrease of the specific capacitance in highly concentrated KOH electrolyte; therefore, it can be deduced that the significant decrease of specific capacitance might be caused by a mismatch between the microstructure of TiC-CDC-1000 and KOH electrolyte.

In order to investigate the relationship between the microstructures of CDCs and KOH electrolyte, TiC-CDC powders synthesized at different temperatures were put in 6 M KOH electrolyte and stirred for 1 h at a speed of 200 rpm, respectively. Thereafter, the produced turbid liquids were stood for 24 h and shown in Fig. 3. It can be seen that all the particles of TiC-CDC-600 sink to the bottom of beaker, indicating that the produced CDC shows a good hydrophilicity in KOH electrolyte (Fig. 3a). When the chlorination temperature increases to 800 °C, besides the bottom, part of the powder float on the surface of KOH electrolyte and the amount of them increases with increasing chlorination temperature (Fig. 3c, e and g). When the chlorination is operated at 1200 °C, nearly all the produced CDC powder floats on the surface of KOH electrolyte (Fig. 3g). It indicates that the produced CDC is very hydrophobic. Fig. 3b, d, f and h show the high-resolution transmission electron microscopy (HRTEM) images of the CDCs synthesized at 600, 800, 1000 and 1200 °C, respectively. It can be seen that the microstructure in TiC-CDC-600 is mainly disordered carbon (Fig. 3b). When the chlorination temperature rises up to 800 °C, many short

and narrow graphite ribbons appear and disperse in disordered carbon (Fig. 3d). When the chlorination temperature further increases to 1000 °C, the produced CDC is mainly composed of short and narrow graphite ribbons (Fig. 3f). In addition, more ordered graphite ribbons are detected in the CDC chlorinated at 1200 °C (denote as TiC-CDC-1200, Fig. 3h). Therefore, it can be deduced that, in KOH electrolyte, the hydrophobicity of the CDCs synthesized at higher temperature might be caused by the appearance of the ordered graphite ribbons.

In order to further investigate the relationship between the microstructure of CDC and KOH electrolyte, FTIR analysis was performed to study the surface properties of the produced CDCs. Fig. 4 shows FTIR spectra of the CDCs synthesized at 600 and 1200 °C. It can be seen from the spectrum of TiC-CDC-600, several characteristic peaks positioned at ~1392, 1459, 1646, 2930 and 3490 cm⁻¹, corresponding to C–C, C–O, C=C, C–H and O–H stretching vibration bends, respectively, are detected. It suggests that there are many carbon dangling bonds and oxygenous functional groups on the surface of the produced CDC. Whereas for TiC-CDC-1200, these characteristic peaks decrease sharply and even invisible for some of them, which might be caused by the increased degree of graphitization. Zheng et al. [20] reported that the introduction of polar oxygen functional groups onto the CDC surface greatly increases the wettability of the material. Therefore, it can be deduced that, in KOH electrolyte, with increasing chlorination temperature, the decreasing hydrophilicity is caused by the decrease of carbon dangling bonds and oxygenous functional groups.

Ethanol, a common dispersing agent, has good affinity with many hydrophobic materials. In order to investigate the effect of

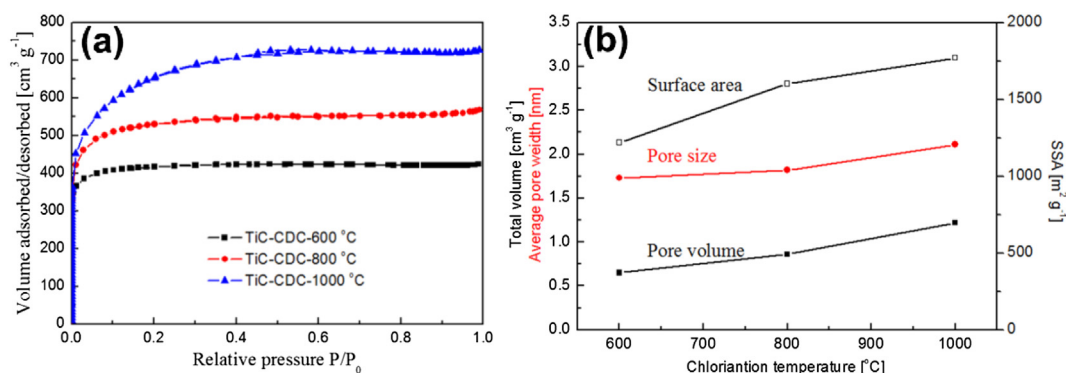


Fig. 2. (a) Nitrogen adsorption/desorption isotherms at 77 K and (b) surface area, pore size and pore volume of CDCs synthesized at different temperatures.

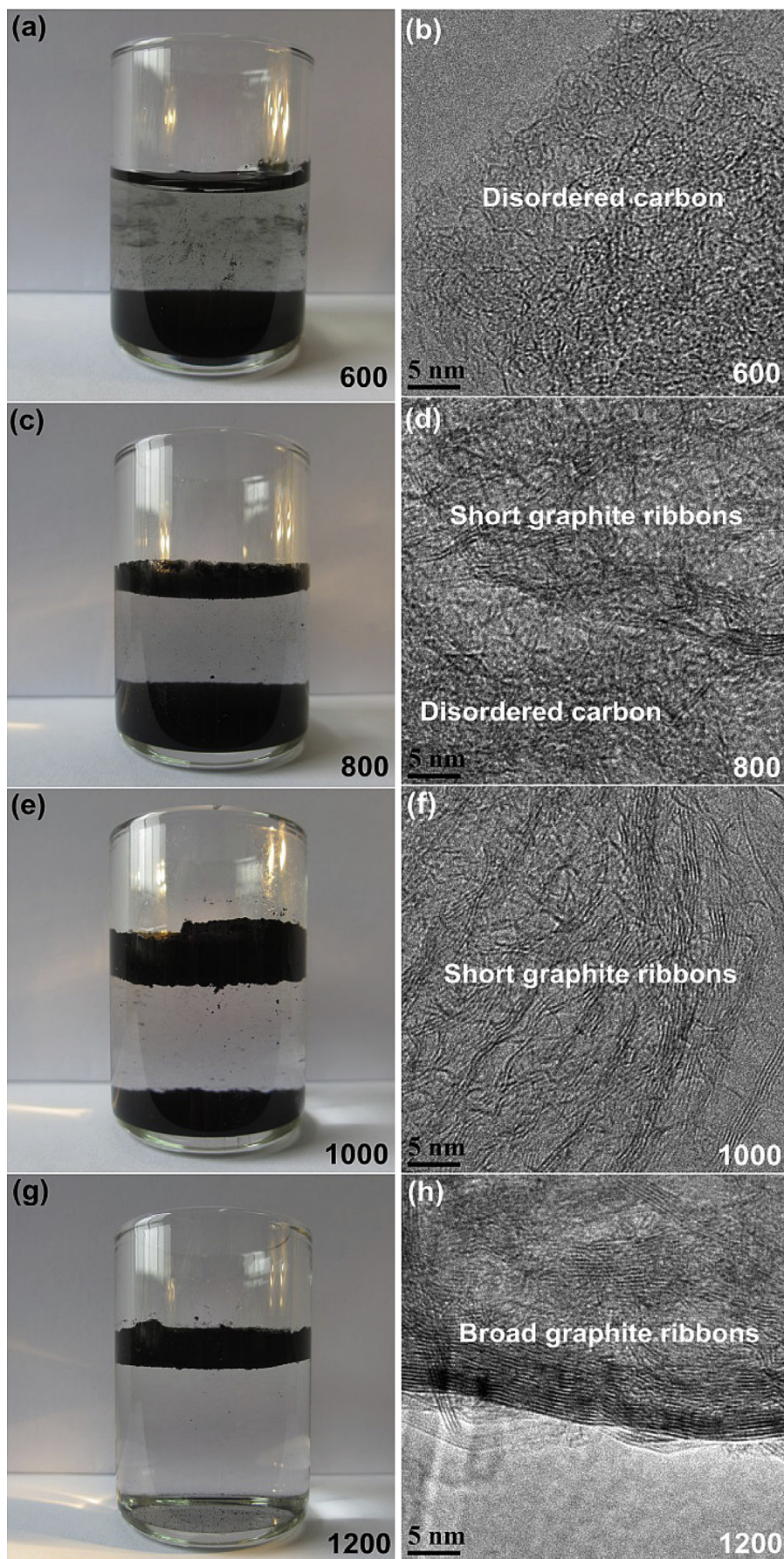


Fig. 3. Optical and HRTEM images of (a, b) TiC-CDC-600, (c, d) TiC-CDC-800, (e, f) TiC-CDC-1000 and (g, h) TiC-CDC-1200. The CDCs are mixed with 6 M KOH solution for optical images.

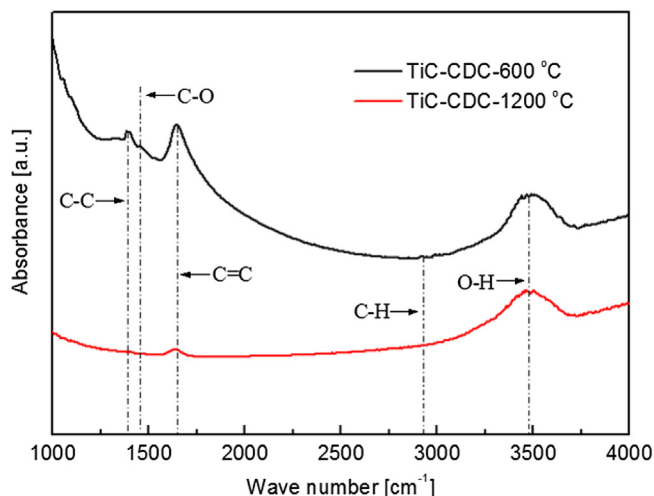


Fig. 4. FTIR spectrum of TiC-CDC-600 and TiC-CDC-1200.

the addition of ethanol to KOH electrolyte on the wettability of the CDCs, the contact angles on TiC-CDCs were measured and shown in Fig. 5. $\sim 10 \mu\text{L}$ 6 M KOH electrolyte or 6 M KOH electrolyte with ethanol (the mass ratio of ethanol to water is 1:9) was dropped on the surfaces of CDCs. It can be found from Fig. 5a–d that the contact angle between KOH drop and TiC-CDC surface increases with increasing chlorination temperature, indicating a decreased wettability. Whereas for KOH with addition of ethanol, all the contact angles are comparable and smaller than those observed in KOH without ethanol, especially for CDCs synthesized at higher temperature (Fig. 5e–h). It suggests that the addition of ethanol to KOH electrolyte can improve the wettability of the TiC-CDCs greatly.

TiC-CDCs are porous materials. Their capacitive behaviors are dependent on the wettability of the inner pores. To further investigate the effect of adding ethanol to KOH electrolyte on the hydrophilicity, TiC-CDC-1200 powder was selected to put in 6 M KOH electrolyte with ethanol and stirred for 1 h at a speed of 200 rpm. Thereafter, the produced turbid liquid was stood for 24 h and shown in Fig. 6a. It can be seen that all the particles of TiC-CDC-1200 sink to the bottom of the beaker, which further indicates that the addition of ethanol in KOH electrolyte improves the wettability of the CDC synthesized at higher temperature greatly. In

addition, when an electrode coated with TiC-CDC-1000 which has been soaked in 6 M KOH electrolyte for a whole week is put in 6 M KOH electrolyte with addition of ethanol, many bubbles appear rapidly and rise to the surface of the electrolyte (Fig. 6b). It indicates that the KOH–ethanol electrolyte can enter and wet the pores of the produced CDC. This observation result agrees well with the contact angle measurements (Fig. 5).

The effect of adding ethanol to KOH electrolyte on the electrochemical performances of the CDCs synthesized at different temperatures was investigated. Both CVs and galvanostatic charge/discharge curves of the produced CDCs measured in 6 M KOH electrolyte with addition of ethanol are shown in Fig. 7. It can be found that the specific capacitance of TiC-CDC-1000 obtained here is much higher than that obtained in aqueous KOH electrolyte (Fig. 1) and comparable with those reported in organic or H_2SO_4 electrolyte [8,11]. It is also found that addition of ethanol leads to a notable increase of specific capacitance of the TiC-CDC-800. This is due to the improved wettability of the hydrophobic graphite. For TiC-CDC-600, addition of ethanol brings a slight increase of specific capacitance (Figs. 1 and 7), which may be caused by some graphite microstructures formed in the region of surface or impurities [31]. Therefore, it can be concluded that the addition of ethanol to aqueous KOH electrolyte is very effective to improve the electrochemical performances of the produced CDCs.

Based on the analysis above, a possible mechanism for the effect of ethanol addition is put forward and schematically shown in Fig. 8. For the CDCs synthesized at higher temperature, the produced graphite is very hydrophobic in aqueous KOH electrolyte, and only the edge of the graphite ribbons can be wetted by the electrolyte. Therefore, large amount of specific surface area among the graphite ribbons cannot be utilized (Fig. 8a), which leads to a sharp decrease of specific capacitance of TiC-CDC-1000 (Fig. 1a). Moreover, the separation of electrolyte and graphite increases internal resistance of the electrode, which leads to a significant IR drop at the beginning of discharge (Fig. 1b). However, it is much easy for KOH electrolyte together with ethanol to enter the pores of the graphite ribbons because ethanol has a good affinity with graphite (Fig. 8b). Moreover, the improved utilization of surface leads to an increase of specific capacitance and a decrease of IR drop (Fig. 7).

The pores in the CDCs synthesized at lower temperature are mainly micropores which are useful for accumulation of charges to obtain high specific capacitance [8]. Whereas the larger pores in the CDCs synthesized at higher temperature are beneficial to provide

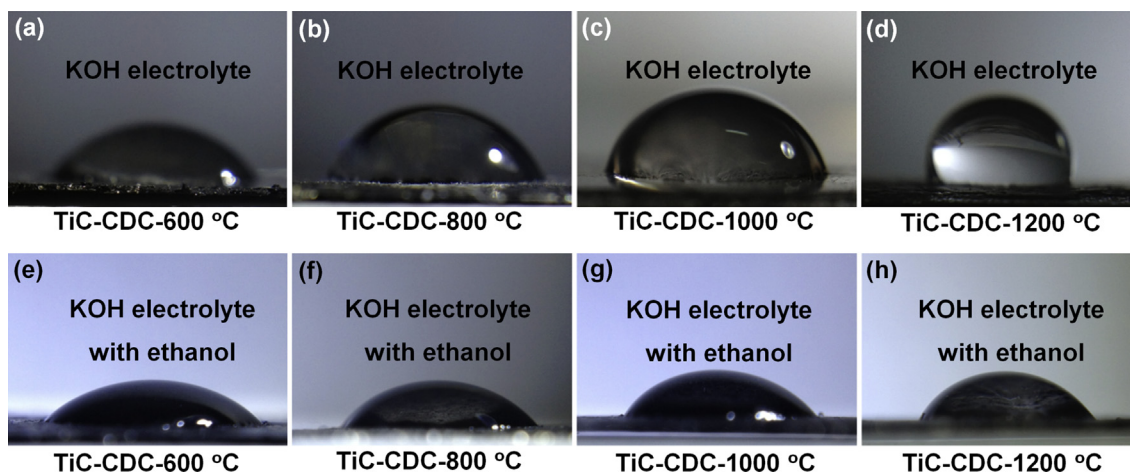


Fig. 5. Optical images of drops of (a–d) 6 M KOH and (e–h) 6 M KOH with ethanol on the surfaces of TiC-CDCs.

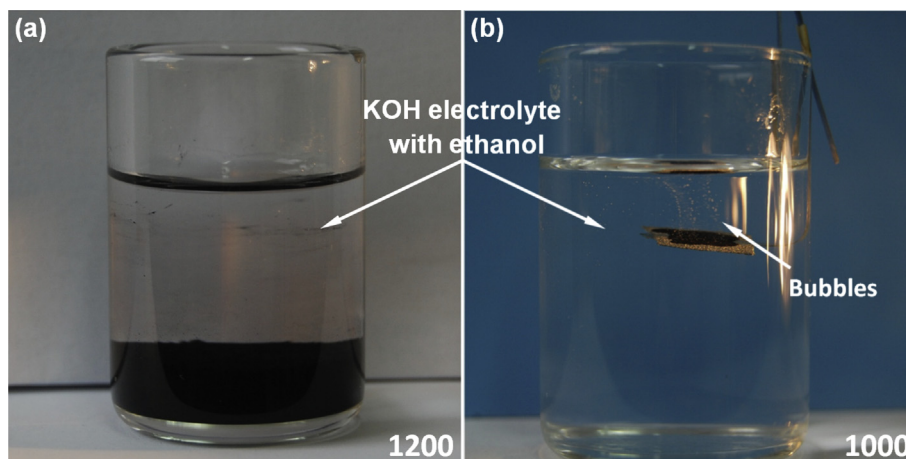


Fig. 6. Optical images of (a) TiC-CDC-1200 powders and (b) electrode coated with TiC-CDC-1000 in 6 M KOH electrolyte with addition of ethanol. The TiC-CDC-1000 electrode was soaked in 6 M KOH for a week before it was put in 6 M KOH with ethanol.

pathways for ion transport [32,33]. But they lead to a decrease of specific capacitance because of the solvated effect [8,11]. Fig. 9 shows the CVs of TiC-CDC-600 at different scan rates in 6 M KOH electrolyte with/without addition of ethanol. It can be found from Fig. 9a that the specific capacitance decreases rapidly with increasing scan rate. Moreover, when the scan rate increases to 200 mV s^{-1} , the rectangular voltammogram cannot be maintained. Whereas for the CVs measured in KOH electrolyte with ethanol (Fig. 9b), the addition of ethanol brings a slight increase of specific capacitance. Further, the voltammogram obtained at scan rate of 200 mV s^{-1} can maintain a quasi-rectangular shape well, which suggests that the addition of ethanol improves the ion transport in the TiC-CDC-600.

TiC-CDC-1000 has different pore structure from TiC-CDC-600. Its scan-rate dependence of specific capacitance is also different from TiC-CDC-600. Fig. 10 shows the CVs of TiC-CDC-1000 at different scan rates in KOH electrolyte with/without addition of ethanol. It can be found from Fig. 10a that the specific capacitance of the CDC in KOH is very low and only a few farads can be gotten even at a very low scan rate (20 mV s^{-1}). Whereas for the CVs measured in 6 M KOH electrolyte with ethanol (the mass ratio of ethanol to water is 1:9), the specific capacitance increases significantly and decreases slowly with increasing scan rate. Moreover, the curve can maintain a quasi-rectangular shape well even at a scan rate of 500 mV s^{-1} and the specific capacitance obtained is larger than that

of TiC-CDC-600 (Fig. 9a), which indicates fast ion transport and excellent capacitive behavior. It is notable that, both SSAs of TiC-CDC-600 and TiC-CDC-1000 are efficiently used in KOH electrolyte with addition of ethanol, but the specific capacitance of TiC-CDC-1000 with higher SSA is still much lower than that of TiC-CDC-600 at lower scan rates. This phenomenon is caused by solvation, which has been reported by Gogotsi et al. [8,11].

Electrochemical impedance spectroscopy (EIS) is used to analyze the characteristic frequency response of CDC-based supercapacitors. Fig. 11a shows AC impedance spectrum (Nyquist plots) for TiC-CDC-600 and TiC-CDC-1000 in 6 M KOH electrolyte with/without addition of ethanol (the mass ratio of ethanol to water is 1:9), respectively. It can be found that the straight line part of TiC-CDC-600 in KOH electrolyte leans more towards the imaginary axis than that of TiC-CDC-1000, which indicates a good capacitive behavior of TiC-CDC-600 in KOH electrolyte. Whereas for the spectrum measured in KOH with ethanol, the straight line part of TiC-CDC-1000 leans to imaginary axis significantly, which means that the addition of ethanol to KOH electrolyte improves its capacitive behavior greatly.

In order to further investigate the electrochemical behavior of the produced CDCs, the impedance spectra at high frequency is shown in Fig. 11a as an inset. As can be seen from the intercept with real axis at high frequency, the resistances of TiC-CDCs in 6 M KOH electrolyte are a little lower than those in 6 M KOH electrolyte with

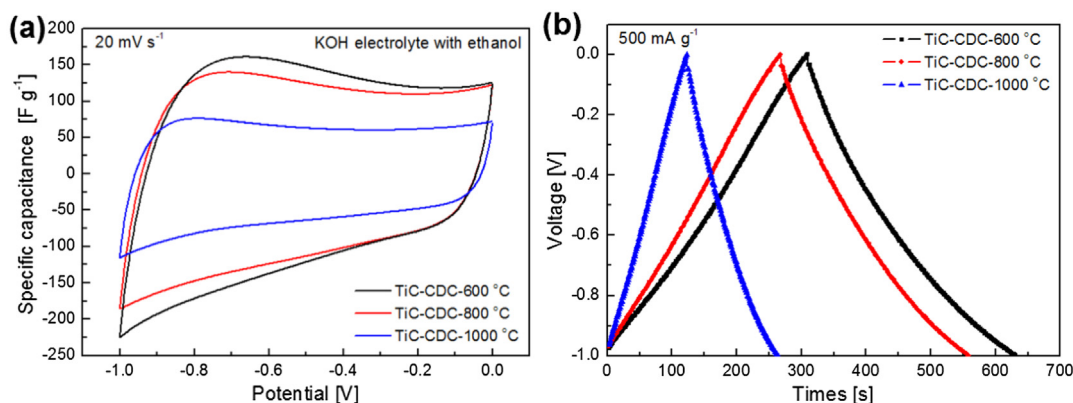


Fig. 7. (a) Cyclic voltammograms (20 mV s^{-1}) and (b) the galvanostatic charging/discharging curves (500 mA g^{-1}) of the CDCs in 6 M KOH aqueous electrolyte with addition of ethanol.

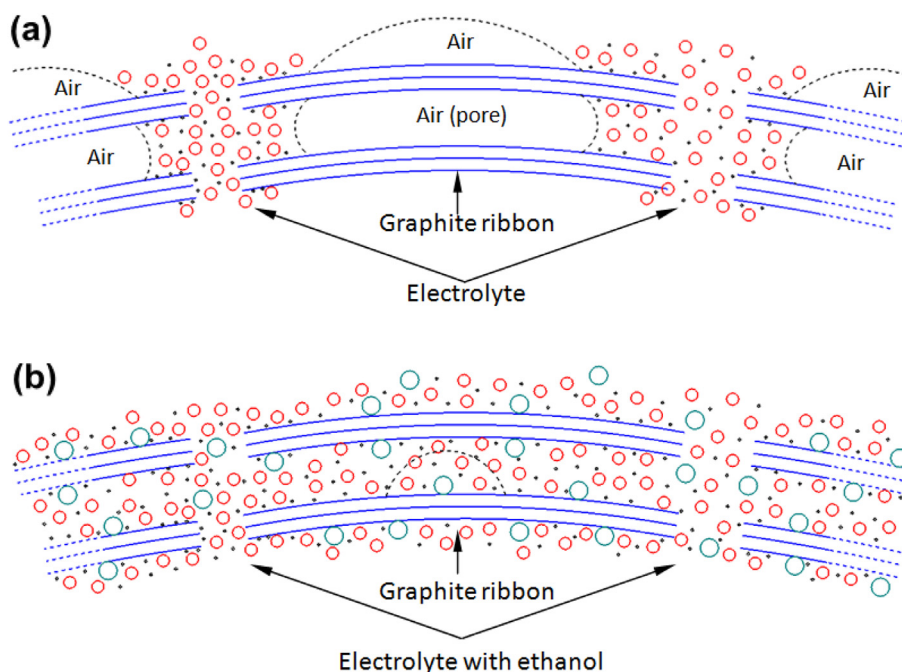


Fig. 8. Schematic diagrams of the CDC synthesized at higher temperature in (a) aqueous KOH electrolyte and (b) KOH electrolyte with addition of ethanol.

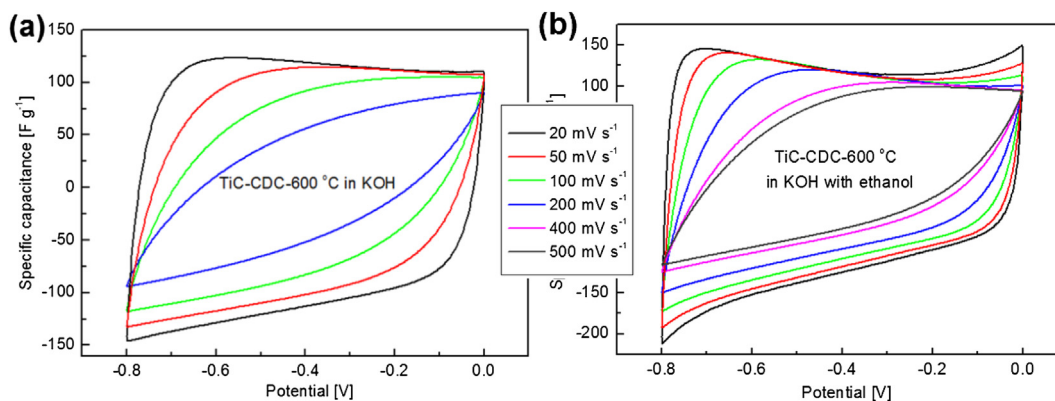


Fig. 9. Cyclic voltammograms of the TiC-CDC-600 in (a) 6 M KOH aqueous electrolyte, and (b) 6 M KOH electrolyte with addition of ethanol at different scan rates.

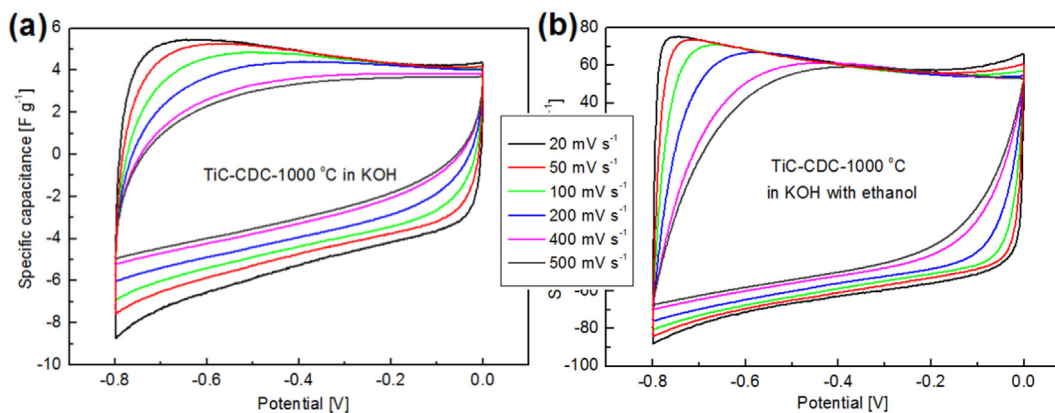


Fig. 10. Cyclic voltammograms of the TiC-CDC-1000 in (a) 6 M KOH aqueous electrolyte, and (b) 6 M KOH electrolyte with addition of ethanol at different scan rates.

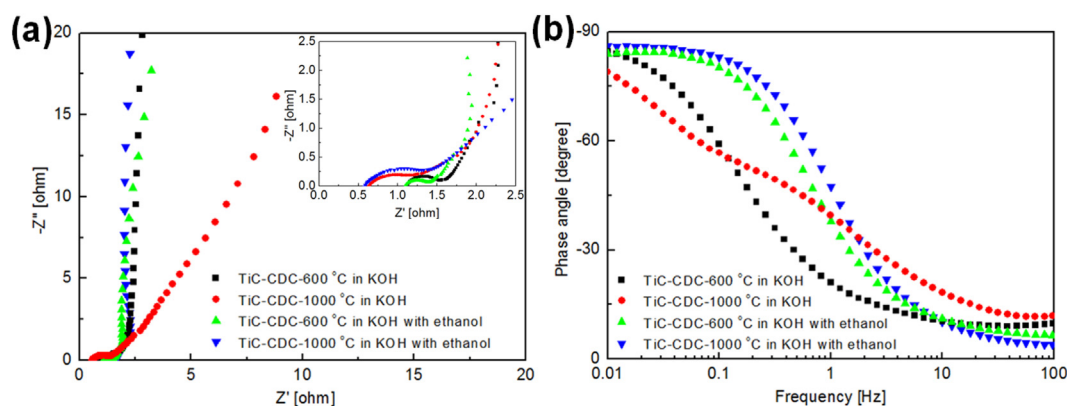


Fig. 11. (a) Nyquist plots and (b) Bode plots of the TiC-CDCs in 6 M KOH electrolyte or in 6 M KOH electrolyte with addition of ethanol (the inset shows expanded high-frequency region of Nyquist plots).

ethanol. In addition, the impedance at high frequency has a special arc-shaped curve. In most cases, the depressed semicircles are considered as small charge-transfer resistances between the electrode and the electrolyte. Therefore, the low charge-transfer resistances for TiC-CDCs in 6 M KOH electrolyte with ethanol might be caused by the improved wettability (Fig. 8). Further, both the slightly decreased specific capacitance and the well maintained quasi-rectangular shape at high scan rate indicate that the charge-transfer resistance has a significant impact on capacitive behavior (Figs. 9 and 10).

Fig. 11b shows the Bode plots of the TiC-CDCs in 6 M KOH electrolyte with/without ethanol, respectively. As can be seen in Fig. 11b, at the same phase angle, the corresponding frequencies of TiC-CDCs in KOH electrolyte with ethanol are higher, indicating a faster ion response time. Moreover, at lower frequency range, the phase angle of TiC-CDC-1000 in KOH electrolyte with ethanol is more close to -90° (ideal value), which might be caused by both the improved wettability and the existence of larger pores in TiC-CDC-1000.

In summary, CDCs synthesized at higher temperature have larger pores which are beneficial to provide pathways for ion transport. But the short and narrow graphite ribbons in the CDC synthesized at higher temperature are very hydrophobic in aqueous KOH electrolyte. The addition of a small amount of ethanol can improve the wettability of graphite effectively, which leads to a sharp increase of the utilization of surface as well as the resultant electrochemical performances.

4. Conclusions

Both the microstructures and the electrochemical performances of the CDCs synthesized from TiC at different temperatures have been investigated. The hydrophilicity of the CDCs in 6 M KOH aqueous electrolyte decreases with increasing chlorination temperatures. The TiC-CDC-1200 exhibits the most hydrophobicity, which is caused by high degree of graphitization, low carbon dangling bonds and less oxygenous functional groups. The electrochemical performances of the CDCs depend on their hydrophilicity in aqueous electrolyte. Lower hydrophilicity of TiC-CDC-1000 leads to a significant decrease of specific capacitance. An addition of small amount of ethanol improves the wettability of the CDCs synthesized at higher temperature greatly as well as the resultant electrochemical performance. The specific capacitance of TiC-CDC-1000 decreases slightly with increasing scan rate and the rectangular voltammogram can be maintained well even at a scan rate of 500 mV s^{-1} . Moreover, The EIS confirms that CDCs synthesized at higher temperature have larger pores which are beneficial to

provide pathways for ion transport. Adding ethanol leads to a sharp increase of the utilization of surface as well as the resultant electrochemical performances. This novel strategy that improving the surface wettability of electrode active material to increase its capacitive behavior can also be applied to other carbon-based supercapacitors.

Acknowledgments

Financial support of this work by National Natural Science Foundation of China (NSFC) under grant No. 50975247 is acknowledged. The authors thank Gold APP Instrument Corporation for the gas sorption analysis.

References

- [1] P. Simon, Y. Gogotsi, *Nat. Mater.* 7 (2008) 845–854.
- [2] Y. Zhang, H. Feng, X. Wu, L. Wang, A. Zhang, T. Xia, H. Dong, X. Li, L. Zhang, *Int. J. Hydrogen Energy* 34 (2009) 4889–4899.
- [3] A. Burke, *J. Power Sources* 91 (2000) 37–50.
- [4] M. Winter, R.J. Brodd, *Chem. Rev.* 104 (2004) 4245–4269.
- [5] J.R. Miller, P. Simon, *Science* 321 (2008) 651–652.
- [6] G. Wang, L. Zhang, J. Zhang, *Chem. Soc. Rev.* 41 (2012) 797–828.
- [7] Y. Zhai, Y. Dou, D. Zhao, P.F. Fulvio, R.T. Mayes, S. Dai, *Adv. Mater.* 23 (2011) 4828–4850.
- [8] J. Chmiola, G. Yushin, Y. Gogotsi, C. Portet, P. Simon, P.L. Taberna, *Science* 313 (2006) 1760–1763.
- [9] S. Kondrat, C.R. Pérez, V. Presser, Y. Gogotsi, A.A. Kornyshev, *Energy Environ. Sci.* 5 (2012) 6474–6479.
- [10] J. Leis, M. Arulepp, M. Käärik, A. Perkson, *Carbon* 48 (2010) 4001–4008.
- [11] C.R. Pérez, S. Yeon, J. Ségolini, V. Presser, P. Taberna, P. Simon, Y. Gogotsi, *Adv. Funct. Mater.* 23 (2013) 1081–1089.
- [12] Y. Gogotsi, A. Nikitin, H. Ye, W. Zhou, J.E. Fischer, B. Yi, H.C. Foley, M.W. Barsoum, *Nat. Mater.* 2 (2003) 591–594.
- [13] M. Kormann, H. Gerhard, N. Popovska, *Carbon* 47 (2009) 242–250.
- [14] J. Chmiola, G. Yushin, R. Dash, Y. Gogotsi, *J. Power Sources* 158 (2006) 765–772.
- [15] G. Yushin, R. Dash, J. Jagiello, J.E. Fischer, Y. Gogotsi, *Adv. Funct. Mater.* 16 (2006) 2288–2293.
- [16] R.K. Dash, G. Yushin, Y. Gogotsi, *Microporous Mesoporous Mater.* 86 (2006) 50–57.
- [17] G.N. Yushin, E.N. Hoffman, A. Nikitin, H. Ye, M.W. Barsoum, Y. Gogotsi, *Carbon* 43 (2005) 2075–2082.
- [18] Y. Zhao, W. Wang, D.B. Xiong, G. Shao, W. Xia, S. Yu, F. Gao, *Int. J. Hydrogen Energy* 37 (2012) 19395–19400.
- [19] A. Jänes, T. Thomborg, H. Kurig, E. Lust, *Carbon* 47 (2009) 23–29.
- [20] L. Zheng, Y. Wang, X. Wang, X. Wang, H. An, L. Yi, *J. Mater. Sci.* 45 (2010) 6030–6037.
- [21] D.N. Futaba, K. Hata, T. Yamada, T. Hiraoka, Y. Hayamizu, Y. Kakudate, O. Tanaike, H. Hatori, M. Yumura, S. Iijima, *Nat. Mater.* 5 (2006) 987–994.
- [22] H. Wu, X. Wang, L. Jiang, C. Wu, Q. Zhao, X. Liu, B. Hu, L. Yi, *J. Power Sources* 226 (2013) 202–209.
- [23] J.P. Zheng, T.R. Jow, *J. Electrochem. Soc.* 144 (1997) 2417–2420.
- [24] J.A. Fernández, M. Arulepp, J. Leis, F. Stoeckli, T.A. Centeno, *Electrochim. Acta* 53 (2008) 7111–7116.

- [25] J.H. Park, O.O. Park, J. Power Sources 111 (2002) 185–190.
- [26] L. Deng, Z. Hao, J. Wang, G. Zhu, L. Kang, Z.H. Liu, Z. Yang, Z. Wang, Electrochim. Acta 89 (2013) 191–198.
- [27] N. Yu, L. Gao, S. Zhao, Z. Wang, Electrochim. Acta 54 (2009) 3835–3841.
- [28] J. Xu, R. Zhang, J. Wang, S. Ge, H. Zhou, Y. Liu, P. Chen, Carbon 52 (2013) 499–508.
- [29] S. Mitani, S.I. Lee, K. Saito, Y. Korai, I. Mochida, Electrochim. Acta 51 (2006) 5487–5493.
- [30] S. Brunauer, L.S. Deming, W.E. Deming, E. Teller, J. Am. Chem. Soc. 62 (1940) 1723–1732.
- [31] Z.G. Cambaz, G.N. Yushin, Y. Gogotsi, K.L. Vyshnyakova, L.N. Pereselenyeva, J. Am. Ceram. Soc. 89 (2006) 509–514.
- [32] M. Rose, Y. Korenblit, E. Kockrick, L. Borchardt, M. Oschatz, S. Kaskel, G. Yushin, Small 7 (2011) 1108–1117.
- [33] H.J. Liu, J. Wang, C.X. Wang, Y.Y. Xia, Adv. Energy Mater. 1 (2011) 1101–1108.